THE PROTEIN SOCIETY

A molecular breadboard: Removal and replacement of subunits in a hepatitis B virus capsid

Lye Siang Lee,[1] Nicholas Brunk,[1,2] Daniel G. Haywood,[3] David Keifer,[3] Elizabeth Pierson,[3] Panagiotis Kondylis,[3] Joseph Che-Yen Wang,[1] Stephen C. Jacobson,[3] Martin F. Jarrold,[3] and Adam Zlotnick [1]*

[1]Molecular and Cellular Biochemistry Department, Indiana University, Bloomington, Indiana 47405
[2]Intelligent Systems Engineering Department, Bloomington, Indiana 47405
[3]Department of Chemistry, Indiana University, Bloomington, Indiana 47405

Received 17 May 2017; Accepted 7 August 2017
DOI: 10.1002/pro.3265
Published online 10 August 2017 proteinscience.org

Abstract: Hepatitis B virus (HBV) core protein is a model system for studying assembly and disassembly of icosahedral structures. Controlling disassembly will allow re-engineering the 120 subunit HBV capsid, making it a molecular breadboard. We examined removal of subunits from partially crosslinked capsids to form stable incomplete particles. To characterize incomplete capsids, we used two single molecule techniques, resistive-pulse sensing and charge detection mass spectrometry. We expected to find a binomial distribution of capsid fragments. Instead, we found a preponderance of 3 MDa complexes (90 subunits) and no fragments smaller than 3 MDa. We also found 90-mers in the disassembly of uncrosslinked HBV capsids. 90-mers seem to be a common pause point in disassembly reactions. Partly explaining this result, graph theory simulations have showed a threshold for capsid stability between 80 and 90 subunits. To test a molecular breadboard concept, we showed that missing subunits could be refilled resulting in chimeric, 120 subunit particles. This result may be a means of assembling unique capsids with functional decorations.

Keywords: self-assembly; nanofluidics; charge detection mass spectrometry; resistive pulse sensing; disassembly

Introduction

Hepatitis B Virus (HBV) is an enveloped virus with an icosahedral capsid. It is an important public health issue: 240 million people have chronic HBV infection and HBV contributes to 780,000 deaths each year.[1–3] HBV also serves as a model system for studying capsid assembly.[4–10] In vitro HBV capsid self-assembly has been studied using the 149-residue assembly domain, Cp149, of the capsid protein. In solution, Cp149 is a dimer that assembles in response to increased ionic strength to predominantly form $T = 4$ (120 dimers) icosahedral capsids; depending on conditions, typically about 5% of capsids are 90-mers with $T = 3$ icosahedral symmetry.[2] During the HBV lifecycle, HBV capsid disassemble to release the viral genome and assemble to

David Keifer's current address is Department of Analytical Sciences, Pharmaceutical Sciences and Clinical Supplies, Merck Research Laboratories, Merck & Co., Inc., Rahway, New Jersey 07065.
Elizabeth Pierson's current address is Department of Chemistry, Salisbury University, 1101 Camden Ave, Salisbury, MD 21801.

Statement: We developed a unique method to generate incomplete crosslinked and uncrosslinked "holey" capsids. We suspect these holey capsids serve as similar to intermediates during disassembly and assembly of the virus particle in vivo and in vitro. Importantly, holes are readily refilled with new subunits allowing orthogonal reactions with different classes of subunit. The same breadboard concept can be applied to other virus structures and nanostructures.

Grant numbers: NIH grant R01 AI118933 to AZ, NSF grant CHE-1308484 to SCJ, and NSF grant CHE-1531823 to MFJ.

*Correspondence to: Adam Zlotnick, Molecular and Cellular Biochemistry Department, Indiana University, Bloomington, Indiana 47405. E-mail: azlotnic@indiana.edu

encapsidate the genome.[11] The mechanisms of disassembly and assembly are not fully understood.[10]

This biological function suggests that it is possible to re-engineer capsid particles, to reversibly remove subunits from intact capsids and to replace them. Studies of dissociation also provide opportunities to examine the stability of an incomplete capsid. To pursue this investigation, we used two single molecule techniques to identify fragments and reassembled capsids, resistive-pulse sensing and charge detection mass spectrometry (CDMS). In a resistive-pulse experiment, solute particles are typically drawn through pores by a potential difference. The translocation of a particle through the pore results in a change in the recorded current (pulse). The amplitude of the current pulse is proportional to the volume of the electrolyte solution displaced from the pore by the translocating particle.[12–16] In-plane nanofluidic devices enable the fabrication of multiple pores connected in series, which increase the resolution of particle size measurements. CDMS is a gas phase technique, where individual ions oscillate in a trap and their mass to charge ratio (m/z) and charge (z) are determined from the frequency and amplitude of the measured signal, respectively.[17]

Properties of virus capsids, symmetry, self-assembly, and their container-like geometry have led to research to develop them as vehicles for nanotechnology.[18,19] Though capsids are built of many subunits, a key feature of modular construction, the ability to swap out components, has not to our knowledge been developed for capsids. In electronics, a breadboard is a chassis where components can readily be inserted and removed to test ciruit design. To develop a virus capsid as a molecular breadboard we want the ability to remove subunits, to access the interior of the capsid, to re-seal the interior cavity, and to re-fill holes with novel subunits. To build a molecular breadboard from HBV capsid protein, we synthesized partially crosslinked and uncrosslinked capsids and used non-denaturing concentrations of urea to remove subunits, leaving holey capsids. After removing subunits, we isolated fragments as small as 90 dimers but smaller particles were not observed in significant amounts. This limit was a surprise as a binomial distribution of species was expected. A non-T = 3 90-mer appears to be a common pause point observed in disassembly reactions and also to play a prominent role in assembly pathways. Critically, we observed that incomplete capsids could further be manipulated and re-filled.

Results

Assembly of hybrid and holey capsids

The protein concentrations of all samples, whether dimer or capsid, are described in terms of the concentration of dimer. To form hybrid capsids, two classes of core protein dimers were required: passivated and non-passivated (Fig. 1). We used a variant of the core protein assembly domain, Cp150, in which the three native cysteines were mutated to alanines and a cysteine was appended to the C-terminus.[20] In capsids, Cp150 dimers can spontaneously crosslink via their C-terminal cysteines (Fig. 1 inset). To prepare passivated Cp150 dimers, incapable of crosslinking, the C-terminal cysteines were blocked with N-ethyl maleimide (NEM) or maleimidyl-BoDIPY-FL, a fluorescent dye. Labeling efficiency of BoDIPY with Cp150 dimer was 1.7–2.0 fluorophores per dimer based on absorbance.[21] The passivated forms are referred to as Cp150.NEM and Cp150.Bo, respectively. Both passivated and non-passivated Cp150 dimers could be driven to assemble into capsids by raising the ionic strength.

Passivated and non-passivated Cp150 were mixed and then assembled by addition of assembly buffer containing NaCl (final concentration of 0.3 M NaCl), in the presence of DTT, to form hybrid particles. Assembly reactions of 1:1, 1:2, 1:3, and 1:4 Cp150.Bo: Cp150 (20 μM total dimer concentration) were investigated over a time course of 24–72 h to ensure maximal assembly. Over time, the free cysteines of non-passivated dimers, adjacent to one another in capsids, crosslinked. Typically, 48 h after initiating assembly, the crosslinked hybrid capsids were tested by non-reducing SDS-PAGE, and ~100% crosslinking was observed (Fig. 1 inset). After 48 h in assembly buffer, hybrid capsids were purified from free dimer by SEC.

Capsids without crosslinks can be dissociated by 3 M urea, whereas 100% Cp150 crosslinked capsids showed no disassembly. We found that in hybrid capsids, where the majority of the dimers were crosslinked, higher urea concentrations were required to remove passivated dimers. Depletion of Cp150.Bo from capsids, measured by absorbance using an HPLC equipped with a multi-wavelength diode array detector, allowed us to follow subunit removal. The 1:2 Cp150.Bo:Cp150 hybrid capsids were mixed with 2–8 M urea and observed at hourly intervals for 24 h by HPLC monitored at 280 and 504 nm (Fig. 2). Absorbance at 504 nm showed maximum removal of Cp150.Bo was achieved with 5 M urea at 2.5 h while leaving capsids otherwise intact. This condition was chosen for the following HPLC experiments.

When a 1:4 Cp150.Bo: Cp150 ratio was used in dissociation experiments, only a small number of dimers were released, and many apparently intact capsids remained [Fig. 2(D)]. Both 1:2 and 1:3 ratios showed a similar number of dimers released per capsid, despite the difference in the amount of passivated dimer added. With a 1:1 ratio, the capsids were not stable to 5 M urea and disassembled into dimers and fragments.

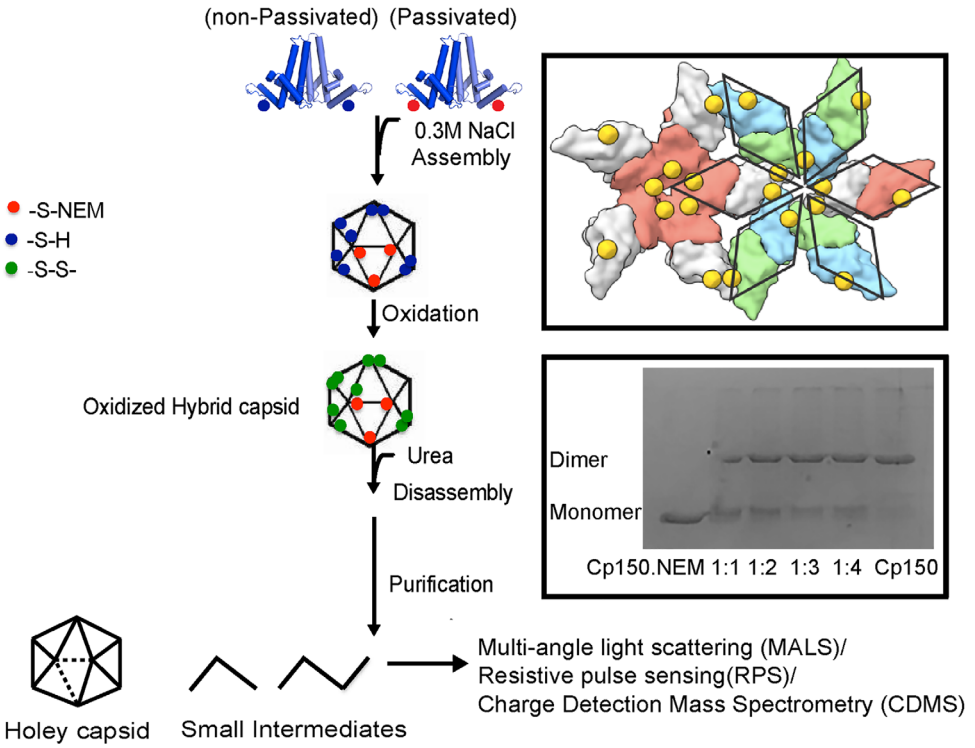

Figure 1. Flowchart of the synthesis and analysis of the holey capsid platform. To form passivated dimers, Hepatitis B Virus (HBV) Cp150 mutant dimers were labeled with N-ethylmaleimide (NEM) to block the only free cysteine present in the mutant. Passivated dimer and non-passivated dimer were mixed and then assembled in 0.5 M NaCl to form $T = 4$ hybrid capsids. The hybrid capsids undergo spontaneous oxidation. To remove passivated dimers, capsids were treated with 5 M urea for 2.5 h. The newly synthesized holey capsids were analyzed by single molecule techniques (e.g., charge detection mass spectrometry (CDMS) and resistive-pulse sensing) and bulk solution techniques. (Inset) Molecular graphic showing cluster of dimers forming a fivefold and quasi-sixfold vertex, viewed from the capsid interior. The AB dimers are red and white; CD dimers are green and blue. The position of residue 142, the last ordered residue in crystal structures, is highlighted by a yellow circle showing how disordered cysteine 150 residues are located where they can form interdimer disulfides. Quasi-sixfold dimers are overlaid with diamonds; these diamond shapes are the basis of the graph theory model used in calculations. SDS-PAGE of hybrid capsids on a non-reducing gel. Cp150 passivated and non-passivated dimers were assembled in 1:1, 1:2, 1:3, and 1:4 ratios, respectively. Uncrosslinked protein runs as a 17 kDa monomer while interdimer crosslinks result in a 35 kDa band

The 1:2 Cp150.Bo: Cp150 hybrid capsids, which had the highest mole percentage of passivated dimer (33%) where incomplete capsid-like complexes remained intact after urea treatment, was chosen for further study.

SEC-MALS, CDMS, and resistive-pulse sensing determined the distribution of the holey capsids

Purified 1:2 hybrid capsids and purified urea-extracted holey capsids were subjected to size exclusion chromatography-multi-angle light scattering SEC-MALS to examine the overall mass distribution of capsids and fragments (Fig. 3). The mass estimated for purified hybrid capsid was 3.8 to 4.2 MDa consistent with a MALS weighted average based on calculated masses for purified capsid of 3.1 MDa for $T = 3$ particles (~10%) and 4.1 MDa for $T = 4$ particles (~90%). The holey capsid yielded a broad bimodal peak unlike the intact capsid control. The masses determined by MALS were distributed from 2.8 to 4 MDa with no smaller material. A wide region of the trailing peak had a mass of approximately 3 MDa. For 1:2 Cp150.Bo:Cp150 capsids, we expected a broad binomial distribution of holey capsids centered at 40 missing dimers per capsid, a species with a mass of 2.7 MDa. To better characterize the disassembly products we examined these reactions by resistive-pulse sensing and CDMS.

CDMS is a single molecule mass spectrometry technique that allows mass determination of individual, megadalton-sized ions in a complex mixture.[17,22,23] The mass (m) of each isolated ion is derived from the simultaneous measurement of mass-to-charge ratio (m/z) and charge (z).[24] SEC purified holey capsids were concentrated and then dialyzed into 0.3 M ammonium acetate, a volatile buffer suitable for CDMS. The observed mass spectrum was dominated by 4 MDa intact $T = 4$ capsids [Fig. 4(A)]. The signal at 3 MDa, 90-dimer complexes, was substantially higher than the typical fraction of $T = 3$ particles formed when assembling hybrid capsids. The signal for incomplete capsids,

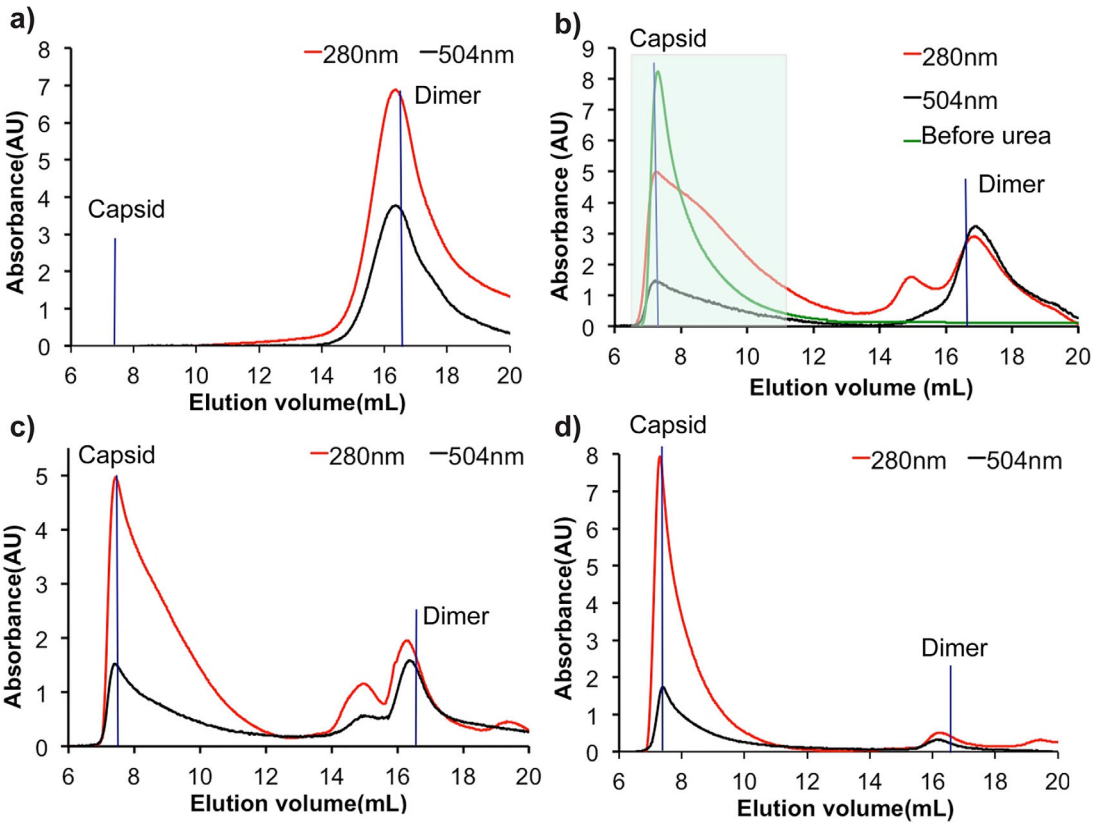

Figure 2. Disassembly conditions for removal of passivated dimers from hybrid capsids. Size exclusion chromatograms show the separation of holey capsids from passivated dimers. Samples had different initial Cp150:Cp150.Bo ratios: (a) 1:1, (b) 1:2, (c) 1:3, (d) 1:4. Absorbance at 280 nm (red) measured protein, absorbance at 504 nm (black) measured solely Cp150.Bo dimers. Substantial Cp150. Bo remained associated with capsid. Hybrid capsids prior to urea extraction of passivated subunits (green line, panel b) elute as a much narrower peak. The box in green in panel identifies the broad peak that was pooled for further analysis

with masses between $T = 3$ and $T = 4$ masses, was lower than expected if on average 1/3 of the subunits were removed by urea. Very few species were observed with masses less than 3MDa. The absence of lower molecular mass species is consistent with SEC-MALS results but could also indicate that smaller Core protein oligomers were lost during preparation or did not have the same efficiency of ionization.

In the resistive-pulse apparatus, the negatively charged HBV particles travel through a series of electrically biased nanopores. As the virus particles transit through the pores, they displace a volume of electrolyte equal to the protein volume. Thus, the amplitude of the current pulse is proportional to the protein volume of the virus particles. The change in current Δi is normalized to the resting current of a given set of nanopores to allow comparison between devices. As controls and calibrants, we measured the current changes induced by $T = 3$ (3 MDa) and $T = 4$ (4 MDa) capsid standards [Fig. 4(B)]. Using these $\Delta i/i$ values as standards, we found that purified holey capsids exhibited a distribution of approximately 50% complete $T = 4$ capsids, 19% intermediate species between $T = 4$ and $T = 3$, and 31% $T = 3$ capsids or similarly sized intermediate species based on count shown in the histogram. We note that ~30 dimers is the lower limit of detection in this experiment set up. Like CDMS, very few intermediates below 3 MDa were observed, and the fraction of 90-dimer particles, overlapping the $T = 3$ peak, was much higher than expected.

These data lead to a working hypothesis that we are accumulating 90-dimer fragments of $T = 4$ capsids and that smaller complexes were depleted. This hypothesis is supported by results from three techniques, SEC-MALS, CDMS, and resistive-pulse sensing. In addition we were surprised to find many intact $T = 4$ capsids in the sample of urea-treated partially crosslinked capsids. This last result is consistent with our observation that not all passivated dimers were removed from hybrid capsids (Fig. 2). Contrary to our initial expectation, a broad distribution of intermediates was expected for 1:2 hybrid capsids where 1/3 of the subunits are passivated. Therefore, we considered how the removal of subunits would affect the distribution of capsids computationally.

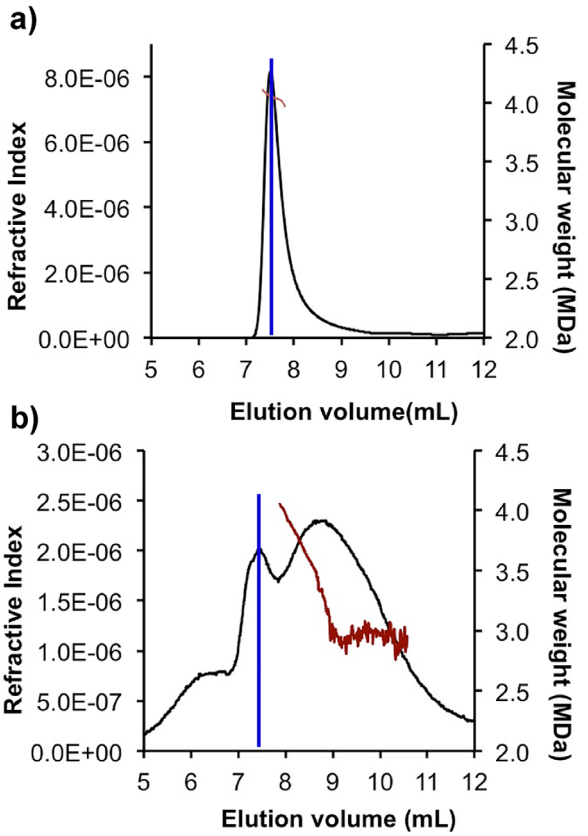

Figure 3. SEC-MALS of (a) intact capsids and (b) capsid fraction of SEC purified holey capsids. Chromatograms show differential refractive index as a function of elution time (black) with molecular masses overlaid (red). The elution volume of capsid is identified by the blue vertical line

The distribution of intermediates correlates with capsid stability and integrity

To simulate the distribution of holey capsids computationally, we built a graph representation of an HBV capsid comprised of 120 nodes (see Fig. 1 inset) and used a Monte Carlo approach to randomly remove nodes (Fig. 5). We assume that in a population of capsids, there will be a stochastic distribution of capsids with different numbers of passivated subunits providing a justification for our Monte Carlo approach to disassembly. In simulations, the complexes with missing nodes were assessed for the number of connections between nodes and whether the remaining nodes formed a single connected graph. We note that these connections are proportional to the net association energy of the capsid.[7] Based on 100,000 disassembly simulations where we evaluated each intermediate in the process of removing one node at a time, we found that as subunits were removed there was a point where capsid integrity failed catastrophically. With the removal of 10 or 20 nodes, essentially all graphs remained intact. When 30 nodes were removed, only 38% of the capsids remained a single graph; the remaining particles broke into two or more smaller graphs. If 40 nodes were removed, nearly all capsids broke down into, on average, three fragments. This model qualitatively matches our experimental observations though it does not precisely fit the details of HBV. Based on the calculations, we would expect to see a distribution of smaller fragments from incomplete graphs.

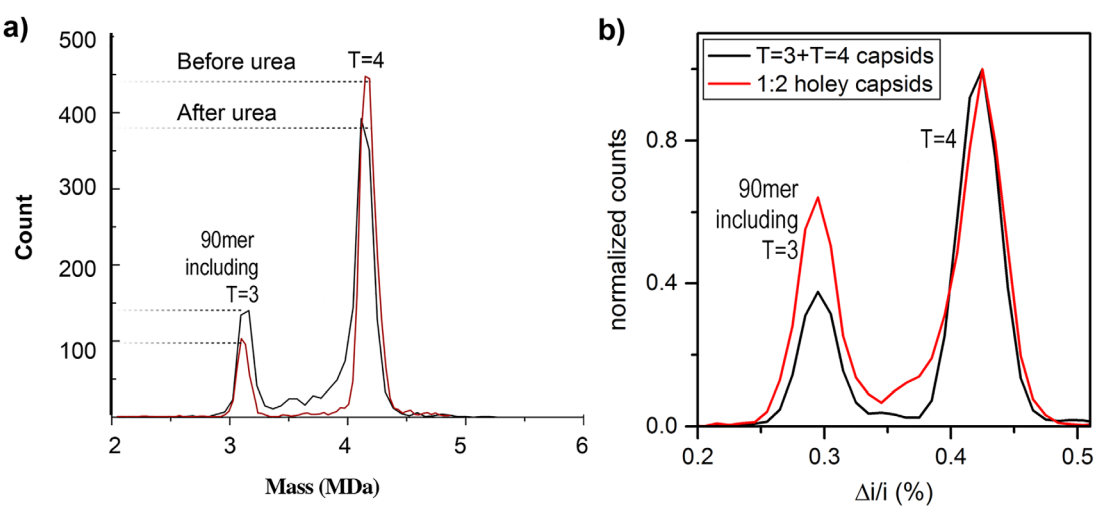

Figure 4. Single molecule analysis of the holey capsids. (a) CDMS histograms of the masses of hybrid and holey capsids. A distribution of intermediates is observed between 90-and 120-dimer complexes. Non-T = 3 90-mers are observed in addition to $T = 3$ capsids. (b) Pulse amplitude histograms from resistive-pulse analysis of holey capsids on a 2-pore device. Pulse amplitudes of the holey capsids (black) overlap with the histogram of mixture $T = 3$ and $T = 4$ (red) capsid standards. Holey capsids include intact $T = 4$ capsids (~50%), intermediates between the $T = 3$ and $T = 4$ standards (~19%), and a mixture of $T = 3$ capsids and similarly sized intermediates (~31%). Resistive-pulse sensing (b) and CDMS (a) presented similar distributions of disassembly products

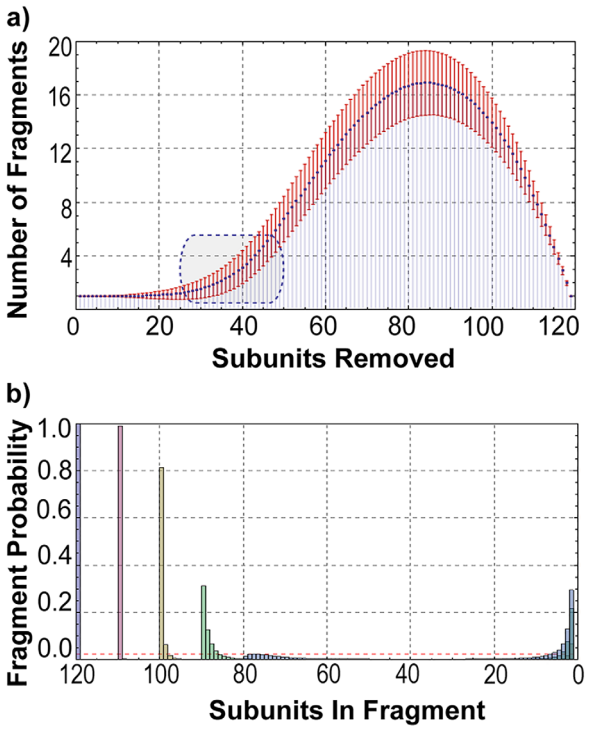

Figure 5. Graph theory analysis shows that removal of ≥30 subunits leads to capsid failure. (a) In Monte Carlo simulations a number of subunits were removed and then the graph was evaluated to determine the average number of fragments (blue points) and the standard deviation (red line); 100,000 simulations were calculated for each number of removed subunits. A graph starts breaking into fragments once the number of removed subunits crosses a threshold of about 30. For less than 30 missing subunits, we see an average of one graph. For greater than 30 missing subunits, we observe an increase in the number of graphs until more than half the subunits are absent from the remaining "fragment". The increase in the probability of fragmentation begins to occur rapidly in the region highlighted by the curved box. (b) A histogram shows the distribution of fragments for graphs with exactly 10 (purple), 20 (pink), 30 (yellow), and 40 (green) missing subunits. For example, with 20 subunits removed, 80% of reactions yield one graph and 5% two graphs. The smaller fragments from these reactions are on the right side of the histogram and have 2 to 5 dimers. With 30 subunits removed, there is a conspicuous increase in fragmentation. When 40 subunits are removed, only a small fraction of capsids remain intact

Taken generally, these results indicate that an intact holey particle with more than 25% of its subunits missing will be unlikely. This leads us to suggest that smaller fragments are depleted from solution perhaps due to rapid dissociation, limited solubility, or aggregation.

Cp149 capsids make non-T = 3 90-mers complexes

The prevalence of non-T = 3 90 dimer disassembly products led us to speculate that they may be uniform, relatively stable complexes. Further supporting this idea, non-T = 3 90-mers have also been observed in assembly reactions.[17] We reasoned that mild dissociation conditions in a capsid unconstrained by crosslinks could yield similar particles. To test this hypothesis, we examined dissociation of Cp149 capsids, which lack any interdimer crosslinking. Cp149 dimers were assembled in high ionic strength ammonium acetate, conditions which enrich the fraction of $T = 4$ particles. These capsids were treated with urea for 1h followed by SEC to remove urea and free dimers. During routine purification of Cp149 we dissociate capsids rapidly and quantitatively with 3 M urea. For Cp149 capsids we found that 1.2 M urea was sufficient to cause partial dissociation. The resulting capsid fractions contained non-T = 3 90-mers, intermediate-sized particles, and complete $T = 4$ capsids determined by resistive-pulse sensing [Fig. 6(A)], very similar to the results observed with crosslinked capsids (see Fig. 4(B)]. Negative stain transmission electron microscopy (TEM) showed a distributions of capsids missing dimers subunits as well as complete $T = 3$ and $T = 4$ capsids. We further examined these particles by TEM using trehalose to minimize distortion of particle ultrastructure during staining [Fig. 6(B)]. Most particles had normal morphology though 5–15% of the particles appeared to have and addition cloud of density. More than 7000 particles were subjected to 2D class averaging. However, we did not observe a class that had an obvious hole or defect suggesting that holey capsids were not uniform did not share a common obvious defect [Fig. 6(D)].

New subunits can be reincorporated into holey capsids

We hypothesized that holey capsids are live polymers, polymers to which new subsuntis can be added. As such, by addition of free dimer they could form the basis for complete patchy particles.[25] To test if we could re-incorporate subunits into holey capsids, we made holey capsids with dimers passivated with non-fluorescent NEM and then determined how much Cp150.Bo could be added. First, we determined conditions where Cp150.Bo did not spontaneously assemble. Cp150.Bo dimers were tested with a titration of salt (10–300 mM NaCl) and protein concentrations (1–10 μM) (Fig. 7). The optimal salt and protein concentrations were determined to be < 7 μM Cp150 at 50 mM NaCl. Holey capsids assembled from 3 μM Cp150 were incubated with 1–6 μM Cp150.Bo dimers for 24 h at 23°C. Samples were tested for backfilling with labeled dimer by SEC. Any absorbance at 504 nm from the BoDIPY moiety that co-eluted with capsid in SEC indicated reconstitution of Cp150.Bo into holey Cp150 capsids to create patchy capsids. As more labeled passivated dimers were added to solution, the capsid peak at 504 nm increased proportionally.

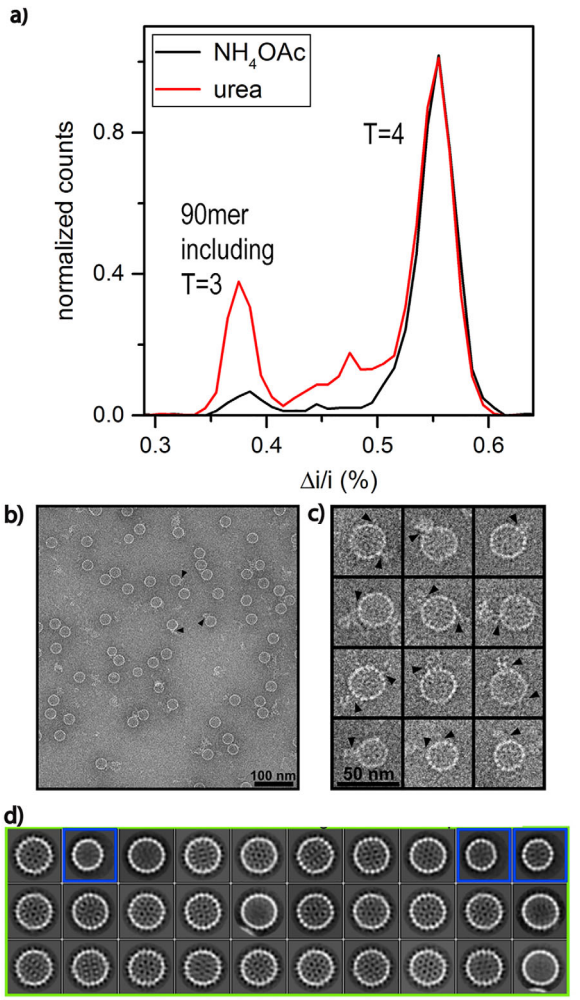

Figure 6. Dissociation of uncrosslinked capsids reveals common disassembly intermediates. Cp149 capsids were partially disassembled in 1.2 M urea. (a) Normalized pulse amplitude histogram from resistive-pulse analysis of holey capsids on a 4-pore device shows that the major peak shifts from 120-mer $T = 4$ capsids to non-T = 3 90-mers. (b) Representative negative stained micrograph of urea treated uncrosslinked capsid. The HBV capsid structure was well preserved by 4% ammonium molybdate plus 0.1% trehalose. No significant flattening effect was observed. In many capsids, a cloud of density was observed connected to the capsid surface (black arrowheads). In this micrograph, 8 of 60 complete particles (~13%) have a cloud and 4 of 60 complete particles (8%) have diameter consistent with $T = 3$ symmetry. (c) Enlarged views of selected capsids show partially detached capsid protein at the capsid surface. (d) Reference-free classification results show no evidence of a hole on the capsid surface, leading us to conclude that the missing subunits are not a continuous patch and may be heterogeneous. The classes in blue boxes have $T = 3$ symmetry.

Also, the capsid peak became narrower and shifted slightly but significantly to the left, suggesting a more homogenous population. The back-filled capsids were further analyzed by CDMS (Fig. 8). CDMS detected a substantial decrease in the relative amount of 90-mer, loss of most intermediates between $T = 3$ and $T = 4$ capsids, and increased intensity of $T = 4$ capsid peak. The residual 90-mer was consistent with the amount of $T = 3$ particles.

Discussion

We have designed a method of forming stable holey capsids by removing passivated dimers from hybrid capsids. The holey capsids are particularly stable to dissociation by urea presumably due to crosslinked subunits. As shown using Cp150.Bo dimers (Fig. 7), holey capsids can be used as a molecular breadboard where subunits can be removed, and new subunits can be installed. In the course of this study we observed a peculiarly large fraction of holey capsids were non-T = 3 90-mers, a species seen during assembly reactions also.[17] Because of the common size, we examined partial dissociation of uncrosslinked Cp149 capsids. We observed a similar distribution of holey capsids including a prevalence of non-T = 3 90-mers. However, we did not observe common features in the Cp149 non-T = 3 90-mers based on 2D class averaging of TEM data.

Similarly, in spite of the random distribution of passivated dimers in hybrid capsids, we did not find a binomial distribution of intermediates. We did not observe any complexes smaller than 90-mers in significant amounts. A graph theory model of subunit removal suggested that removal of subunits beyond a threshold of about 1/4 of the graph leads to fragmentation of particles into unstable or insoluble aggregates that could not be readily isolated; this model is essentially a molecular realization of the Jenga game where players remove pieces from a complex structure until the structure collapses.

The prevalence of non-T = 3 90-mers during disassembly may arise from the biophysics of HBV capsid structure or the topology of icosahedral geometry. Non-T = 3 90-mers are also observed during assembly.[17] We note the absence of smaller fragments and speculate that the many exposed interaction surfaces on the edges of these complexes will make them susceptible to aggregation, effectively removing them from solution. As non-T = 3 90-mers are not a uniform species, small holes are randomly distributed and create a fenestrated capsid surface; evidence is contrary to the possibility that subunits are removed as a continuous block to form a single, large hole. We will continue to investigate whether these incomplete capsids are a peculiarity of HBV or general feature of $T = 4$ geometry.

We were unable to remove all of the passivated dimers. One explanation for this behavior is that when a passivated dimer is surrounded by crosslinked subunits, which should be more common when passivated dimers are at low mole fraction (e.g., 1:4 capsids), that they cannot be removed; whereas clusters of passivated dimers found in 1:1, 1:2, and 1:3 capsids are susceptible to urea (Fig. 2). Isolated passivated dimers may be resistant to

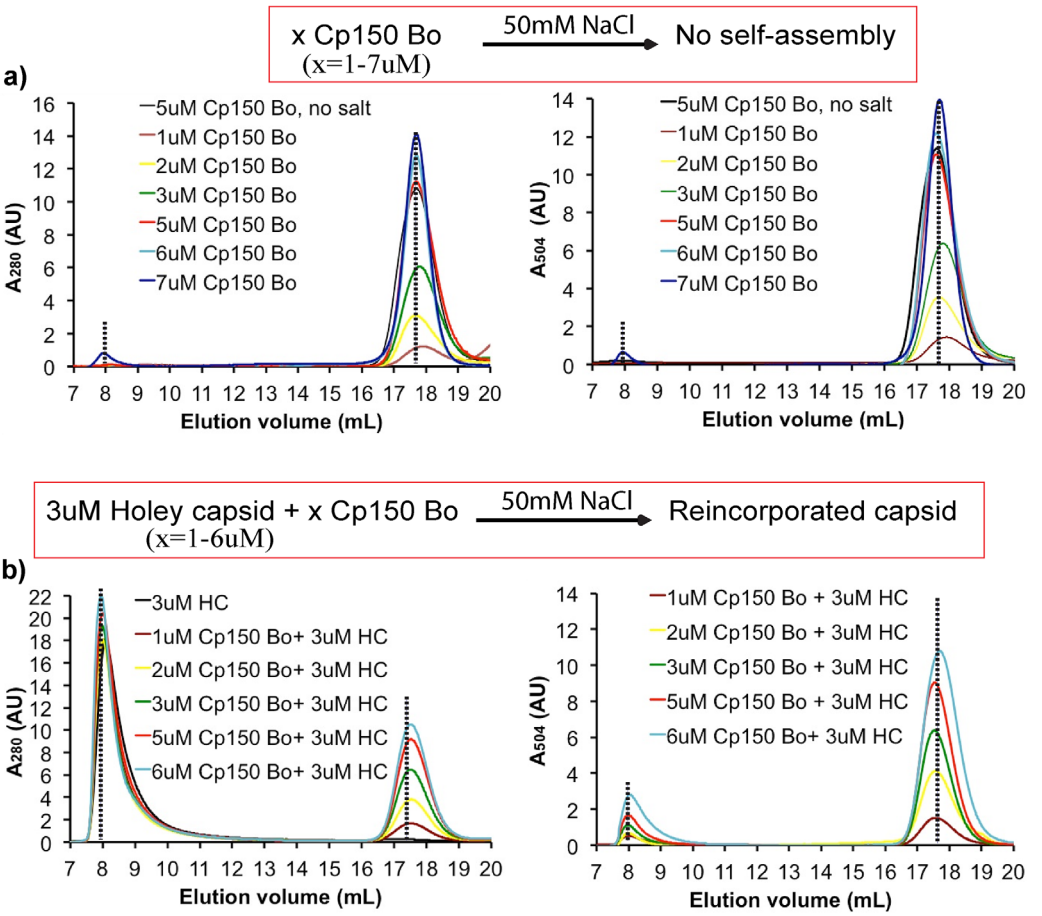

Figure 7. SEC chromatograms of holey capsids back-filled with new Cp150.Bo dimers. Chromatographs are shown for absorbance measured at 280 nm (left side) to accentuate protein absorbance and at 504 nm for BoDIPY absorbance (right). (a) Cp150.Bo dimers at $\leq$6 μM do not assemble in 50 mM NaCl. (b) Chromatograms of 1–6 μM Cp150.Bo dimer mixed with 3 μM unlabeled holey capsids show absorbance at 504 nm, indicating that labeled dimers were incorporated into holey capsids

dissociation from capsids because each dimer must break four contacts. Conversely, clusters of dimers would require breaking only three or two contacts per dimer to the contiguous shell. This same rationale may explain why subunits in capsids only rarely exchange with free subunits.[26]

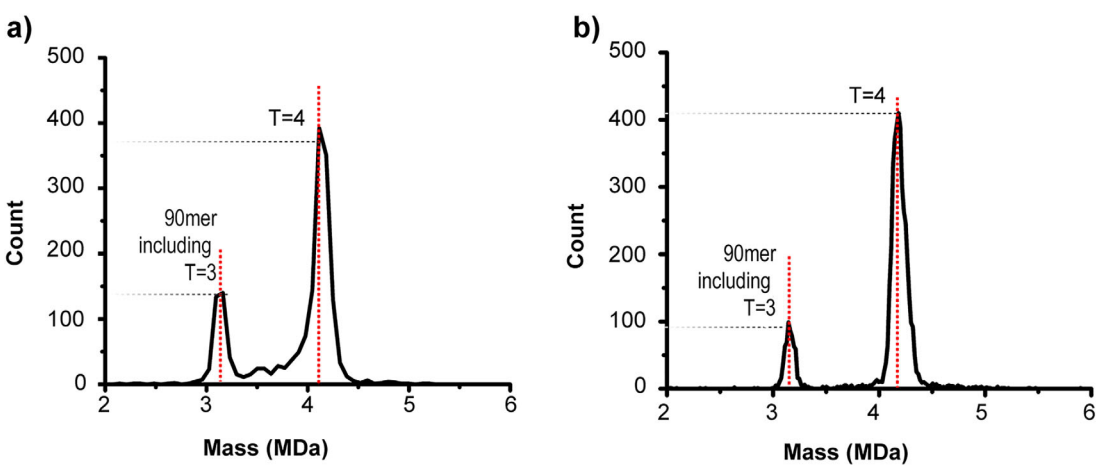

Figure 8. Single molecule analysis of back-filled holey capsids by CDMS. Mass spectra of (a) purified holey capsid (5 μM dimer concentration) after disassembly and purification [Fig. 4(A)] and (b) after incubation with 6 μM Cp150.Bo dimer in 50 mM NaCl. These data indicate that intermediates observed in (a) have incorporated new subunits leading the $T = 4$ capsid signal to increase

Single molecule, high resolution techniques were required to define the distribution of intermediates in this system. Bulk method like SEC-MALS can be misleading as they describe an average value of the overall distribution and would never have revealed the accumulation of non-T = 3 90-mers. The two fundamentally distinct single particle techniques used in this investigation showed a remarkable consistency.

Finally, in this study we were able to isolate incomplete particles, crosslinked and uncrosslinked. We were able to backfill crosslinked particles with chemically modified subunits. Unlike a strategy of of mixing diverse subunits together, using holey capsids provides a means for addressing, emptying, or filling a capsid. It also allows one to backfill a capsid with subunits that form stronger or weaker inter-subunit interactions, a strategy that may not always work in a mixed assembly. A long-term goal of this study is to provide a means of incorporating modularity into a virus capsid to incorporate novel specificity, chemical markers, cargoes, and sensors into a self-assembling nanometer-sized complex.[18]

Materials and Methods

Preparation of protein for hybrid capsids

For uniformity, the protein concentration of all samples, whether dimer or capsid, are described in terms of the concentration of dimer. Cp150 mutant dimers were purified using a previously reported protocol.[21] Cp150 was passivated by labeling the C-terminal cysteine with N-ethylmaleimide (Cp150.NEM) or the fluorescent dye BoDIPY-FL (Cp150.Bo) as previously described,[27] except that the excess NEM was removed by dialysis instead of with a desalting column. The ratio of BoDIPY label per Cp150 dimer was determined by absorbance.[21] The efficiency of labeling with NEM or BoDIPY-FL was demonstrated by showing that subunits in capsids did not form disulfide crosslinks; capsids comprised of passivated dimers were treated with 3M urea which led to complete dissociation to dimers.[28]

Reduced Cp149/Cp150 dimers were purified using a previously reported protocol.[9,27] Cp149 dimers were dialyzed into 200 mM ammonium acetate and allowed to assemble into capsids overnight at room temperature. Cp149 capsids were then purified from remaining dimer. Purified capsids (1μM dimer concentration) were disassembled by incubation with 1.2 M urea for 1 h. After disassembly, these capsids are purified from dimers and diluted into a final concentration of 1 M NaCl and analyzed further by resistive-pulse sensing on 4-pore devices. Reduced Cp150 dimers were assembled in 0.3M NaCl into capsids for 8 h. Reduced 150 capsids were then purified from remaining dimer. Purified capsids (1μM dimer concentration) were disassembled by incubation with 1.2 M urea for 1 h. After disassembly, these reduced Cp150 capsids are purified and oxidized before analyzed by TEM.

Disassembly conditions determined by size exclusion chromatography analysis

Assembled hybrid capsids were tested for optimal disassembly conditions over a matrix of urea concentration (2–8 M) and time (1–24 h). Reactions were evaluated by separation over a Superose 6 size exclusion chromatography (SEC) column on a Shimadzu HPLC equipped with a diode array detector and monitored at 280 nm and 504 nm. The capsid fraction, separated from smaller intermediates, was concentrated to 5 μM dimer for subsequent resistive-pulse sensing, CDMS, and size exclusion chromatography-multi-angle light scattering (SEC-MALS) analyses.

Sec-Mals

For SEC-MALS, samples were resolved over a Superose 6 column and evaluated with a Dawn Heleos light scattering detector and an Optilab REX refractive index detector (both from Wyatt, Santa Barbara, CA). Data were analyzed with the manufacturer's software. BSA (5 mg/mL) was used as a standard for normalizing instrument parameters with the 50 mM $NaHCO_3$ buffer used. A dn/dc refractive index increment of 0.185 ml/g was used for protein in these calculations. After disassembly reactions, the capsid fraction was first purified by SEC, and then a 5 μM 100 μL sample was injected onto the SEC-MALS instrument.

Resistive-pulse sensing

Nanofluidic devices for resistive-pulse sensing were fabricated as previously described.[29] Briefly, two, closely spaced V-shaped microchannels were etched to a depth of 9.6 ± 0.1 μm in a borosilicate glass substrate. A focused ion beam (Auriga 60, Carl Zeiss, Inc.) milled directly into the glass a nanochannel with three or four nanopores in series to bridge the gap between the two microchannels. The nanopores were milled as single lines with a 30 kV beam at 20 pA and a dose of 0.011 μC/μm and were 295 ± 5 nm long, 63 ± 4 nm wide, and 62 ± 6 nm deep. The nanochannels, connecting the nanopores, were milled with a 30 kV beam at 50 pA and a dose of 0.5 nC/μm^2 and were 1.04 ± 0.02 μm or 0.503 ± 0.008 μm long for the 3- and 4-pore devices, respectively, 339 ± 0.6 nm wide, and 111 ± 0.5 nm deep. The nanochannels, connecting the nanopores with the microchannels, were milled with a 30 kV beam at 50 pA and a dose of 1.0 nC/μm^2 and were 532 ± 8 nm wide and 224 ± 2 nm deep.

To complete the devices, milled substrates and #1.5 cover slips were hydrolyzed with 1 M NaOH for 15 min, sonicated in water, brought into contact

while wet, dried overnight at 90°C, and annealed at 545°C for 12 h. The bonded channels were rinsed sequentially with water, 1 M NaOH, and water for 15 min before buffer was drawn into the channels by vacuum.

For resistive-pulse measurements, channels were filled with 50 mM HEPES buffer (pH 7.5) with 1 M NaCl. Capsid samples (diluted to 1 μM dimer concentration) in the same buffer were drawn into one of the microchannels by vacuum. Then, an Axopatch 200B (Molecular Devices, LLC) was used to apply a potential through silver-silver chloride electrodes across the nanochannel and drive the capsids electrokinetically through the pores. All data were collected at ~17 nA current baseline, with a 40 kHz sampling frequency and a 10 kHz filter frequency. Data were analyzed with a modified version of Open Nanopore 1.2 in Matlab to detect and measure pulse amplitudes and to determine times between adjacent pulses. Times between pulses were fitted to a lognormal distribution, and pulses separated by ≤ 3 ms of the mean time were designated as pulse sequences, corresponding to a single capsid passing through the three or four nanopores. Capsid amplitudes were calculated as the average amplitude of each pulse sequence.

Charge detection mass spectrometry

Details of the home-built charge detection mass spectrometer (CDMS) have been given elsewhere.[24] Briefly, ions were generated by nano-electrospray ionization. They were transmitted through three stages of differential pumping and then energy analyzed. Ions with a narrow band of kinetic energies are focused into an electrostatic ion trap where the trapped ions oscillate back and forth through a metal tube. The charge induced on the tube is detected by a charge sensitive preamplifier. The resulting signal is amplified, digitized, and analyzed by fast Fourier transforms. Only results from single ion trapping events are retained. The mass to charge ratio (m/z) is obtained from the oscillation frequency, and the charge is determined from the magnitude of the fundamental peak. Multiplying the m/z and charge gives the mass. The process is repeated for thousands of ions, and the results are binned into a mass spectrum. For the 91 ms trapping time used here, the relative root-mean-square uncertainty in mass ($\Delta m/m$, where Δm is the standard deviation of the mass measurement) is expected to be ~0.013. Samples analyzed with CDMS were buffer exchanged by spin-column SEC (Bio-Rad Laboratories, Inc.) into 100 mM NH_4OAc.

Monte Carlo simulations of dissociation

Dissociation products as a function of the number of subunits removed were calculated with a disassembly Monte Carlo algorithm written in Mathematica 10.2.0 (Wolfram Research). The virus particle was expressed as a regular graph of size v_{tot} from which an arbitrarily sized subset of vertices was removed.[30] A representation of a fragment of this graph is shown in Figure 1, $v_{tot} = 120$ and the vertices, like HBV dimers, are 4 regular. This approach is analogous to removal of passivated dimer from capsid. Analysis of the remaining set of vertices ($v_{rem} = v_{tot} - v_{\varepsilon}$) allows prediction of the results of experiment. Fragmentation of the graph representing a capsid is defined as formation of two or more subsets of connected vertices. Sequential averaging of 100,000 simulations produced the point-wise fragmentation curve. A more complete analysis of dissociation using this model will appear in a subsequent paper.

Image analysis of non-*T* = 3 90-mers

To minimize the particle collapse caused by conventional negative stain specimen preparation, we modified the procedures to embed the HBV particles in a thick layer of stain. 300-mesh cooper grids covered with continous carbon film (EMS) were glow-discharged for 15 s. Approximately 4 μl of sample solution was applied to the grid for 25 s. Excess solution was blotted, and the grid was then inverted onto a 100 μl drop of negative stain (4% (w/v) ammonium molybdate, 1% (w/v) trehalose at pH 7) for 10 s. Excess stain was removed, and the grid allowed to air dry. Samples were imaged using a JEOL 3200FS electron microscope operating under low-dose conditions ($\leq$20 $e^-/Å^2$) to minimize beam induced damage. Images were collected at a nominal magnification of 60,000x with a Gatan 895 CCD camera. Particle extraction and contrast transfer function estimation were performed with EMAN2 software.[31] A phase corrected particle set was generated and imported into Relion (v1.4) for 2D classification.[32]

Acknowledgments

We gratefully acknowledge the facilities and staff of the Indiana University-Bloomington Electron Microscopy Center. AZ has an interest in a biotech company that may be considered a conflict of interest.

References

1. Seeger C, Zoulim F, Mason WS, Hepadnaviruses. In: Knipe DM, Griffin DE, Lamb RA, Martin MA, Roizman B, Straus SE, Eds. (2007) Fields virology. Philadelphia: Lippincott Williams & Wilkins, pp. 2977–3029.
2. Selzer L, Zlotnick A, Assembly and release of Hepatitis B virus. In: Seeger C, Locarnini S, Eds. (2014) Hepatitis B and delta viruses. New York: Cold Spring Harbor Press.
3. Gish R, Given BD, Lai C-L, Locarnini S, Lau JYN, Lewis DL, Schluep T (2015) Chronic hepatitis B: natural history, virology, current management and a glimpse at future opportunities. Antiviral Res 121:47–58.

4. Zlotnick A (2005) Theoretical aspects of virus capsid assembly. J Mol Recognit 18:479–490.
5. Bourne C, Finn MG, Zlotnick A (2006) Global structural changes in hepatitis B capsids induced by the assembly effector HAP1. J Virol 80:11055–11061.
6. Bourne CR, Katen SP, Fulz MR, Packianathan C, Zlotnick A (2009) A mutant hepatitis B virus core protein mimics inhibitors of icosahedral capsid self-assembly. Biochemistry 48:1736–1742.
7. Katen SP, Zlotnick A (2009) Thermodynamics of virus capsid assembly. Methods Enzymol 455:395–417.
8. Burns K, Mukherjee S, Keef T, Johnson JM, Zlotnick A (2010) Altering the energy landscape of virus self-assembly to generate kinetically trapped nanoparticles. Biomacromolecules 11:439–442.
9. Packianathan C, Katen SP, Dann CE, 3rd, Zlotnick A (2010) Conformational changes in the Hepatitis B virus core protein are consistent with a role for allostery in virus assembly. J Virol 84:1607–1615.
10. Selzer L, Kant R, Wang JC, Bothner B, Zlotnick A (2015) Hepatitis B virus core protein phosphorylation sites affect capsid stability and transient exposure of the C-terminal domain. J Biol Chem 290:28584–28593.
11. Grimm D, Thimme R, Blum HE (2011) HBV life cycle and novel drug targets. Hepatology Intl 5:644–653.
12. Harms ZD, Mogensen KB, Nunes PS, Zhou K, Hildenbrand BW, Mitra I, Tan Z, Zlotnick A, Kutter JP, Jacobson SC (2011) Nanofluidic devices with two pores in series for resistive-pulse sensing of single virus capsids. Anal Chem 83:9573–9578.
13. Haywood DG, Harms ZD, Jacobson SC (2014) Electro-osmotic flow in nanofluidic channels. Anal Chem 86: 11174–11180.
14. Harms ZD, Haywood DG, Kneller AR, Selzer L, Zlotnick A, Jacobson SC (2015) Single-particle electrophoresis in nanochannels. Anal Chem 87:699–705.
15. Haywood DG, Saha-Shah A, Baker LA, Jacobson SC (2015) Fundamental studies of nanofluidics: nanopores, nanochannels, and nanopipets. Anal Chem 87:172–187.
16. Kondylis P, Zhou Z, Harms ZD, Kneller AR, Lee LS, Zlotnick A, Jacobson SC (2017) Nanofluidic devices with 8 pores in series for real-time, resistive-pulse analysis of hepatitis B virus capsid assembly. Anal Chem 89:4855–4862.
17. Pierson EE, Keifer DZ, Selzer L, Lee LS, Contino NC, Wang JC, Zlotnick A, Jarrold MF (2014) Detection of late intermediates in virus capsid assembly by charge detection mass spectrometry. J Am Chem Soc 136: 3536–3541.
18. Douglas T, Young M (2006) Viruses: making friends with old foes. Science 312:873–875.
19. Mateu MG (2016) Assembly, engineering and applications of virus-based protein nanoparticles. Adv Exp Med Biol 940:83–120.
20. Zlotnick A, Cheng N, Stahl SJ, Conway JF, Steven AC, Wingfield PT (1997) Localization of the C terminus of the assembly domain of hepatitis B virus capsid protein: implications for morphogenesis and organization of encapsidated RNA. Proc Natl Acad Sci USA 94:9556–9561.
21. Zlotnick A, Lee A, Bourne CR, Johnson JM, Domanico PL, Stray SJ (2007) In vitro screening for molecules that affect virus capsid assembly (and other protein association reactions). Nat Protoc 2:490–498.
22. Kukreja AA, Wang JC, Pierson E, Keifer DZ, Selzer L, Tan Z, Dragnea B, Jarrold MF, Zlotnick A (2014) Structurally similar woodchuck and human hepadnavirus core proteins have distinctly different temperature dependences of assembly. J Virol 88:14105–14115.
23. Chen C, Wang JC, Pierson EE, Keifer DZ, Delaleau M, Gallucci L, Cazenave C, Kann M, Jarrold MF, Zlotnick A (2016) Importin beta can bind hepatitis B virus core protein and empty core-like particles and induce structural changes. PLoS Pathog 12:e1005802.
24. Contino NC, Jarrold MF (2013) Charge detection mass spectrometry for single ions with a limit of detection of 30 charges. Int J Mass Spect 345–347:153–159.
25. Jiang S, Chen Q, Tripathy M, Luijten E, Schweizer KS, Granick S (2010) Janus particle synthesis and assembly. Adv Mater 22:1060–1071.
26. Uetrecht C, Watts NR, Stahl SJ, Wingfield PT, Steven AC, Heck AJ (2010) Subunit exchange rates in Hepatitis B virus capsids are geometry- and temperature-dependent. Phys Chem Chem Phys 12:13368–13371.
27. Stray SJ, Johnson JM, Kopek BG, Zlotnick A (2006) An in vitro fluorescence screen to identify antivirals that disrupt hepatitis B virus capsid assembly. Nat Biotechnol 24:358–362.
28. Singh S, Zlotnick A (2003) Observed hysteresis of virus capsid disassembly is implicit in kinetic models of assembly. J Biol Chem 278:18249–18255.
29. Harms ZD, Selzer L, Zlotnick A, Jacobson SC (2015) Monitoring assembly of virus capsids with nanofluidic devices. ACS Nano 9:9087–9096.
30. Buldyrev SV, Parshani R, Paul G, Stanley HE, Havlin S (2010) Catastrophic cascade of failures in interdependent networks. Nature 464:1025–1028.
31. Tang G, Peng L, Baldwin PR, Mann DS, Jiang W, Rees I, Ludtke SJ (2007) EMAN2: an extensible image processing suite for electron microscopy. J Struct Biol 157:38–46.
32. Scheres SH (2012) RELION: implementation of a Bayesian approach to cryo-EM structure determination. J Struct Biol 180:519–530.